Label-free sensitivity of long-period gratings enhanced by atomic layer deposited TiO_2 nano-overlays

Mateusz Smietana,[1,6] Marcin Koba,[3,*] Ewa Brzozowska,[4] Krzysztof Krogulski,[1] Jakub Nakonieczny,[1] Lukasz Wachnicki,[5] Predrag Mikulic,[2] Marek Godlewski,[5] and Wojtek J. Bock[2]

[1]*Institute of Microelectronics and Optoelectronics, Warsaw University of Technology, Koszykowa 75, Warsaw 00-662, Poland*

[2]*Centre de recherche en photonique, Université du Québec en Outaouais, 101 rue Saint-Jean-Bosco, Gatineau, QC, J8X 3X7, Canada*

[3]*National Institute of Telecommunications, Szachowa 1, Warsaw, 04-894, Poland*

[4]*Institute of Immunology and Experimental Therapy, Polish Academy of Science, Weigla 12,Wroclaw, 53-114, Poland*

[5]*Institute of Physics, Polish Academy of Science, Al. Lotnikow 32/46,Warsaw, 02-668, Poland*

[6]*M.Smietana@elka.pw.edu.pl*

[*]*mkoba@elka.pw.edu.pl*

Abstract: In this paper, we discuss an impact of thin titanium dioxide (TiO_2) coatings on refractive index (RI) sensitivity and biofunctionalization of long-period gratings (LPGs). The TiO_2 overlays on the LPG surfaces have been obtained using atomic layer deposition (ALD) method. This method allows for a deposition of conformal, thickness-controlled, with well-defined optical properties, and high-RI thin films which are highly desired for optical fiber sensors. It has been found that for LPGs working at a dispersion turning point of higher order cladding modes only tens of nanometers of TiO_2 overlay thickness allow to obtain cladding mode transition effect, and thus significant improvement of RI sensitivity. When the TiO_2 overlay thickness reaches 70 nm, it is possible to obtain RI sensitivity exceeding 6200 nm/RIU in RI range where label-free sensors operate. Moreover, LPGs with TiO_2-enhanced RI sensitivity have shown improved sensitivity to bacteria endotoxin (*E. coli* B lipopolysaccharide) detection, when TiO_2 surface is functionalized with endotoxin binding protein (adhesin) of T4 bacteriophage.

OCIS codes: (050.2770) Gratings; (060.2370) Fiber optics sensors; (240.0310) Thin films; (280.1415) Biological sensing and sensors; (280.4788) Optical sensing and sensors; (310.3840) Materials and process characterization.

References and links

1. C.-H. Yeh, C.-W. Chow, J.-Y. Sung, P.-C. Wu, W.-T. Whang, and F.-G. Tseng, "Measurement of organic chemical refractive indexes using an optical time-domain reflectometer," Sensors (Basel Switzerland) **12**(12), 481–488 (2012).
2. A. M. Vengsarkar, P. J. Lemaire, J. B. Judkins, V. Bhatia, T. Erdogan, and J. E. Sipe, "Long-period fiber gratings as band-rejection filters," J. Lightwave Technol. **14**(1), 58–65 (1996).
3. V. Bhatia, "Applications of long-period gratings to single and multi-parameter sensing," Opt. Express **4**(11), 457–466 (1999).
4. I. M. Ishaq, A. Quintela, S. W. James, G. J. Ashwell, J. M. Lopez-Higuera, and R. P. Tatam, "Modification of the refractive index response of long period grating using thin film overlays," Sens. Actuators B Chem. **107**(2), 738–741 (2005).
5. Z. Gu and Y. Xu, "Design optimization of a long-period fiber grating with sol–gel coating for a gas sensor," Meas. Sci. Technol. **18**(11), 3530–3536 (2007).
6. D. Galbarra, F. J. Arregui, I. R. Matias, and R. O. Claus, "Ammonia optical fiber sensor based on self-assembled zirconia thin films," Smart Mater. Struct. **14**(4), 739–744 (2005).

#233817 - $15.00 USD Received 2 Feb 2015; revised 13 Mar 2015; accepted 16 Mar 2015; published 24 Mar 2015

7. H. Kim, H.-B.-R. Lee, and W.-J. Maeng, "Applications of atomic layer deposition to nanofabrication and emerging nanodevices," Thin Solid Films **517**(8), 2563–2580 (2009).
8. R. E. Sah, R. Driad, F. Bernhardt, L. Kirste, C.-C. Leancu, H. Czap, F. Benkhelifa, M. Mikulla, and O. Ambacher, "Mechanical and electrical properties of plasma and thermal atomic layer deposited Al_2O_3 films on GaAs and Si," J. Vac. Sci. Technol. A **31**(4), 041502 (2013).
9. R. L. Puurunen, "Surface chemistry of atomic layer deposition: A case study for the trimethylaluminium/water process," J. Appl. Phys. **97**(12), 121301 (2005).
10. M. Smietana, J. Szmidt, M. L. Korwin-Pawlowski, W. J. Bock, and J. Grabarczyk, "Application of diamond-like carbon films in optical fibre sensors based on long-period gratings," Diamond Related Materials **16**(4–7), 1374–1377 (2007).
11. M. Smietana, W. J. Bock, P. Mikulic, and J. Chen, "Pressure sensing in high-refractive-index liquids using long-period gratings nanocoated with silicon nitride," Sensors (Basel) **10**(12), 11301–11310 (2010).
12. K. Krogulski, M. Śmietana, B. Michalak, A. K. Dębowska, M. Dudek, B. S. Witkowski, P. Mikulic, and W. J. Bock, "Properties of diamond-like carbon nano-coating deposited with RF PECVD method on UV-induced long-period fibre gratings," Phys. Status Solidi-A **211**(10), 2307–2312 (2014).
13. L. Martinu and D. Poitras, "Plasma deposition of optical films and coatings: A review," J. Vac. Sci. Technol. A **18**(6), 2619–2645 (2000).
14. M. Śmietana, M. Mysliwiec, P. Mikulic, B. S. Witkowski, and W. J. Bock, "Capability for fine tuning of the refractive index sensing properties of long-period gratings by atomic layer deposited Al_2O_3 overlays," Sensors (Basel Switzerland) **13**(12), 16372–16383 (2013).
15. E. Davies, R. Viitala, M. Salomaki, S. Areva, L. Zhang, and I. Bennion, "Sol–gel derived coating applied to long-period gratings for enhanced refractive index sensing properties," J. Opt. A, Pure Appl. Opt. **11**(1), 015501 (2009).
16. U. Diebold, "The surface science of titanium dioxide," Surf. Sci. Rep. **48**(5–8), 53–229 (2003).
17. N. Ghrairi and M. Bouaicha, "Structural, morphological and optical properties of TiO_2 thin films synthesized by the electrophoretic deposition technique," Nanoscale Res. Lett. **7**(1), 357 (2012).
18. R. C. Jayasinghe, A. G. U. Perera, H. Zhu, and Y. Zhao, "Optical properties of nanostructured TiO_2 thin films and their application as antireflection coatings on infrared detectors," Opt. Lett. **37**(20), 4302–4304 (2012).
19. M. R. Saleem, P. Stenberg, T. Alasaarela, P. Silfsten, M. B. Khan, S. Honkanen, and J. Turunen, "Towards athermal organic-inorganic guided mode resonance filters," Opt. Express **19**(24), 24241–24251 (2011).
20. T. Alasaarela, T. Saastamoinen, J. Hiltunen, A. Säynätjoki, A. Tervonen, P. Stenberg, M. Kuittinen, and S. Honkanen, "Atomic layer deposited titanium dioxide and its application in resonant waveguide grating," Appl. Opt. **49**(22), 4321–4325 (2010).
21. H. Chen, Z. Guc, and K. Gao, "Humidity sensor based on cascaded chirped long-period fiber gratings coated with TiO2/SnO2 composite films," Sensor. Actuat, B.-Chem. **196**, 18–22 (2014).
22. M. Consales, G. Berruti, A. Borriello, M. Giordano, S. Buontempo, G. Breglio, A. Makovec, P. Petagna, and A. Cusano, "Nanoscale TiO_2-coated LPGs as radiation-tolerant humidity sensors for high-energy physics applications," Opt. Lett. **39**(14), 4128–4131 (2014).
23. R.-Z. Yang, W.-F. Dong, X. Meng, X.-L. Zhang, Y.-L. Sun, Y.-W. Hao, J.-C. Guo, W.-Y. Zhang, Y.-S. Yu, J.-F. Song, Z.-M. Qi, and H.-B. Sun, "Nanoporous TiO2/Polyion Thin-Film-Coated Long-Period Grating Sensors for the Direct Measurement of Low-Molecular-Weight Analytes," Langmuir **28**(23), 8814–8821 (2012).
24. M. Hernáez, I. Del Villar, C. R. Zamarreño, F. J. Arregui, and I. R. Matias, "Optical fiber refractometers based on lossy mode resonances supported by TiO_2 coatings," Appl. Opt. **49**(20), 3980–3985 (2010).
25. L. Coelho, D. Viegas, J. L. Santos, and J. M. M. M. de Almeida, "Enhanced refractive index sensing characteristics of optical fibre long period grating coated with titanium dioxide thin films," Sensor. Actuat, B.-Chem. **202**, 929–934 (2014).
26. K. Krogulski, M. Śmietana, B. Michalak, A. K. Dębowska, M. Szymańska, Ł. Wachnicki, S. Gierałtowska, M. Godlewski, P. Mikulic, and W. J. Bock, "Effect of TiO2 nano-overlays deposited with atomic layer deposition on refractive index sensitivity of long-period gratings," Int. J. Smart Sens. Int. Syst. **7**, 573–577 (2014).
27. A. Cusano, A. Iadicicco, P. Pilla, L. Contessa, S. Campopiano, A. Cutolo, and M. Giordano, "Mode transition in high refractive index coated long period gratings," Opt. Express **14**(1), 19–34 (2006).
28. K. Zhou, H. Liu, and X. Hu, "Tuning the resonant wavelength of long period fiber gratings by etching the fiber's cladding," Opt. Commun. **197**(4–6), 295–299 (2001).
29. P. Pilla, C. Trono, F. Baldini, F. Chiavaioli, M. Giordano, and A. Cusano, "Giant sensitivity of long period gratings in transition mode near the dispersion turning point: an integrated design approach," Opt. Lett. **37**(19), 4152–4154 (2012).
30. M. Smietana, W. J. Bock, P. Mikulic, A. Ng, R. Chinnappan, and M. Zourob, "Detection of bacteria using bacteriophages as recognition elements immobilized on long-period fiber gratings," Opt. Express **19**(9), 7971–7978 (2011).
31. M. A. Ali, S. Srivastava, P. R. Solanki, V. V. Agrawal, R. John, and B. D. Malhotra, "Nanostructured anatase-titanium dioxide based platform for application to microfluidics cholesterol biosensor," Appl. Phys. Lett. **101**(8), 084105 (2012).
32. H. Shafiee, E. A. Lidstone, M. Jahangir, F. Inci, E. Hanhauser, T. J. Henrich, D. R. Kuritzkes, B. T. Cunningham, and U. Demirci, "Nanostructured Optical Photonic Crystal Biosensor for HIV Viral Load Measurement," Sci. Rep. **4**, 4116 (2014).

#233817 - $15.00 USD Received 2 Feb 2015; revised 13 Mar 2015; accepted 16 Mar 2015; published 24 Mar 2015

33. E. Brzozowska, M. Śmietana, M. Koba, S. Górska, K. Pawlik, A. Gamian, and W. J. Bock, "Recognition of bacterial lipopolysaccharide using bacteriophage-adhesin-coated long-period gratings," Biosens. Bioelectron. **67**, 93–99 (2015).
34. F. Höök, J. Voros, M. Rodahl, R. Kurrat, P. Boni, J. J. Ramsden, M. Textor, N. D. Spencer, P. Tengvall, J. Gold, and B. Kasemo, "A comparative study of protein adsorption on titanium oxide surfaces using in situ ellipsometry, optical waveguide lightmode spectroscopy, and quartz crystal microbalance/dissipation," Coll. Surf. B **24**(2), 155–170 (2002).
35. P. Hengen, "Purification of His-Tag fusion proteins from Escherichia coli," Trends Biochem. Sci. **20**(7), 285–286 (1995).
36. L. Nieba, S. E. Nieba-Axmann, A. Persson, M. Hämäläinen, F. Edebratt, A. Hansson, J. Lidholm, K. Magnusson, A. F. Karlsson, and A. Plückthun, "BIACORE analysis of histidine-tagged proteins using a chelating NTA sensor chip," Anal. Biochem. **252**(2), 217–228 (1997).
37. M. Koba, M. Smietana, E. Brzozowska, S. Gorska, P. Mikulic, and W. J. Bock, "Reusable Bacteriophage Adhesin-coated Long-period Grating Sensor for Bacterial Lipopolysaccharide Recognition," J. Lightwave Technol., http://ieeexplore.ieee.org/xpl/articleDetails.jsp?arnumber=6930716.
38. P. J. Lemaire, R. M. Atkins, V. Mizrahi, and W. A. Reed, "High pressure H_2 loading as a technique for achieving ultrahigh UV photosensitivity and thermal sensitivity in GeO_2 doped optical fibers," Electron. Lett. **29**(13), 1191–1193 (1993).
39. T. Erdogan, V. Mizrahi, P. J. Lemaire, and D. Monroe, "Decay of ultraviolet-induced fiber Bragg gratings," J. Appl. Phys. **76**(1), 73–80 (1994).
40. M. Myśliwiec, J. Grochowski, K. Krogulski, P. Mikulic, W. J. Bock, and M. Smietana, "Effect of wet etching of arc induced long-period gratings on their refractive index sensitivity," Acta Phys. Pol. A **124**(3), 521–524 (2013).
41. M. Smietana, W. J. Bock, and J. Szmidt, "Evolution of optical properties with deposition time of silicon nitride and diamond-like carbon films deposited by radio-frequency plasma-enhanced chemical vapor deposition method," Thin Solid Films **519**, 6339–6343 (2011).
42. M. Smietana, W. J. Bock, J. Szmidt, and J. Grabarczyk, "Substrate effect on the optical properties and thickness of diamond-like carbon films deposited by the RF PACVD method," Diamond Related Materials **19**(12), 1461–1465 (2010).
43. M. Smietana, W. J. Bock, and P. Mikulic, "Temperature sensitivity of silicon nitride nanocoated long-period gratings working in various surrounding media," Meas. Sci. Technol. **22**(11), 115203 (2011).
44. X. Shu, L. Zhang, and I. Bennion, "Sensitivity characteristics of long period fiber gratings," J. Lightwave Technol. **20**(2), 255–266 (2002).
45. S. G. Bartual, J. M. Otero, C. Garcia-Doval, A. L. Llamas-Saiz, R. Kahn, G. C. Fox, and M. J. van Raaij, "Structure of the bacteriophage T4 long tail fiber receptor-binding tip," Proc. Natl. Acad. Sci. U.S.A. **107**(47), 20287–20292 (2010).
46. P. Pilla, A. Sandomenico, V. Malachovská, A. Borriello, M. Giordano, A. Cutolo, M. Ruvo, and A. Cusano, "A protein-based biointerfacing route toward label-free immunoassays with long period gratings in transition mode," Biosens. Bioelectron. **31**(1), 486–491 (2012).
47. P. Pilla, V. Malachovská, A. Borriello, A. Buosciolo, M. Giordano, L. Ambrosio, A. Cutolo, and A. Cusano, "Transition mode long period grating biosensor with functional multilayer coatings," Opt. Express **19**(2), 512–526 (2011).</jrn>

1. Introduction

Numerous of chemical and biological substances can be detected by measurement of refractive index (RI) of their liquid solutions, e.g [1]. That is why RI sensors have a wide range of applications in chemistry, food industry, and biochemistry. Such sensors are expected to provide high sensitivity to RI of external medium and immediate response. Sensors based on long-period gratings (LPGs) can easily meet these requirements. The LPG is a structure typically made by periodic (period Λ of 100 to 700 μm) modulation of refractive index within core of a single-mode optical fiber [2]. The modulation induces coupling between core mode and *m* cladding modes resulting in appearance of a series of resonance attenuation peaks in LPG's transmission spectrum [3]. These resonance wavelengths λ^m are defined by (1), where n_{eff}^{co} and $n_{eff}^{cl,m}$ are effective refractive indices of core and m^{th} order cladding mode, respectively.

$$\lambda^m = \left(n_{eff}^{co} - n_{eff}^{cl,m}\right)\Lambda \tag{1}$$

The value of $n_{eff}^{cl,m}$ depends on the external RI (n_{ext}), and thus the latter has a direct influence on spectral response of the LPG. Namely, the increase of n_{ext} increases $n_{eff}^{cl,m}$ and

#233817 - $15.00 USD Received 2 Feb 2015; revised 13 Mar 2015; accepted 16 Mar 2015; published 24 Mar 2015

finally induces the resonant wavelength shift toward shorter wavelengths, e.g [3]. The effect gets stronger when n_{ext} is closer to that of cladding, which is typically made of fused silica (n_D = 1.458 RIU). However, it has been shown that coating LPG with high-refractive index (high-*n*) overlay leads to shift of the highest RI sensitivity range towards its lower values [4]. Such modification depends on overlay thickness and its optical properties, mainly refractive index. The most popular methods for tuning the RI response through the use of nano-coatings are based on immersing the LPGs in a liquid precursor. Some of the liquid-precursor-based deposition techniques are Langmuir-Blodgett [4], sol-gel [5], and electrostatic self-assembly (ESA) [6]. However, these methods do not provide efficient control of properties of the overlays or are very time consuming. To overcome some of the mentioned disadvantages the Atomic Layer Deposition (ALD) can be used as an alternative. It belongs to a group of chemical vapor deposition (CVD) methods, and allows for the deposition of thin films on various substrates with atomic scale precision [7]. Thus, the ALD gives precise control of the overlay properties on whole length of the grating. The method is based on the gas-solid reactions occurring at the surface of substrate and belongs to a group of layer-by-layer techniques. The majority of ALD reactions use two chemicals, usually called precursors. The growth of films with ALD typically includes four steps: exposure of the surface to the first precursor, purge of the reaction chamber to remove the non-reacted precursors and the gaseous reaction by-products, exposure to the second precursor, and again purge or evacuation of the reactor chamber. The surface reactions can be accomplished using thermal chemistry or with the assistance of plasma [8]. The process temperature depends on the precursor and is typically in the range of 30 to 150 °C [9]. The major limitation of ALD is its low growth rate. However, the growth rate can be compensated by the increased size of the reactor and the deposition of multiple samples.

In our previous works we reported results on modification of the RI response of the LPG-based sensors with hard and high-*n* overlays deposited from gas precursors with a radio-frequency plasma-enhanced chemical-vapor-deposition (RF PECVD) method [10–12]. The properties of the films can be easily changed over a wide range of refractive index values by varying the gas composition and other deposition parameters [13]. However, the control of the film thickness in nanometer range and symmetrical deposition around the fiber with this method are still challenging. Moreover, we also investigated modification of RI response of the LPG with deposition of Al_2O_3 overlay with ALD method [14]. Since Al_2O_3 belongs to a group of relatively low-refractive-index materials (*n* at λ = 1550 nm reaches 1.62 RIU), the thickness of the deposited overlay must be high (over 200 nm for optimal thickness at $n_{ext} \approx 1.3330$ RIU) in order to effectively tune RI sensitivity of the devices [15]. For such thick overlays long ALD processes are required, which may be both time consuming and expensive.

In this paper we present detail investigation of high-*n* titanium dioxide (TiO_2) thin overlays applied as both improvement of the RI sensitivity and interfacing with bio-overlay. TiO_2 shows high temperature and high electrical resistance as well as high hardness, low optical absorption, and biocompatibility [16,17]. It has been used as an antireflection coating on infrared detectors [18], optical resonance filters [19] or as planar waveguiding structures [20]. It has been shown that when TiO_2 overlay is deposited on LPG with sol-gel method it adsorbs water molecules and can be applied for humidity sensing [21,22]. Also nanoporous ESA deposited TiO_2/polyion overlay on LPGs has been used for low-molecular-weight chemicals detection [23]. Refractive index of these sol-gel and ESA deposited material is typically below 2 [15,23,24]. When uniform and non-porous TiO_2 overlay is deposited, e.g., using evaporation by electron beam, the LPG can be applied for RI sensing [25]. In this work high-*n* TiO_2 is deposited on LPGs surface with the use of ALD technique [26]. The TiO_2 films are applied for fine tuning of spectral properties of the LPGs, and in consequence their RI sensitivity. In this experiment we deposited the overlays on LPGs working at dispersion

#233817 - $15.00 USD Received 2 Feb 2015; revised 13 Mar 2015; accepted 16 Mar 2015; published 24 Mar 2015

turning point (DTP), where the highest sensitivity can be obtained [27,28]. Presented study of a few different TiO_2 coatings gives dipper experimental insight into resonance behavior at the vicinity of DTP. Moreover, combining effect of DTP and higher order cladding mode transition induced by deposition on the overlay allows for maximizing sensitivity of the LPG, especially in RI range employed by label-free biosensors [29,30]. It has been shown that surface of TiO_2 can be functionalized with a number of molecules, which bind to it by electrostatic [31] or chemical [32] interaction. In this paper we report evidences of successful TiO_2 surface biofunctionalization with green fluorescent protein and for a first time bacteriophage adhesins, i.e., proteins capable for specific binding of bacteria or its endotoxins, i.e., lipopolysaccharide (LPS) [33]. It has been shown that proteins can physically adsorb to TiO_2 surface [34]. Furthermore, in this work chemical TiO_2 surface functionalization with nickel ions and histidine-tagged proteins have been applied. Polyhistidine-tags are one of the most popular systems used for affinity purification of polyhistidine-tagged recombinant proteins expressed in *Escherichia coli* and other prokaryotic expression systems [35]. The system is also used in BIACORE analysis of proteins using a chelating NTA sensor chip [36]. Selective binding of His-tagged protein to Nickel ions allows relatively easy and quick acquisition of the desired protein preparation or its immobilization to a surface. Moreover the system allows for the sensor's regeneration [37].

2. Experimental details

2.1 LPG manufacturing

In this experiment we used commercially available germanium-doped Corning SMF-28 single-mode optical fiber. High pressure hydrogen loading has been used to increase photosensitivity of the fiber [38]. A set of LPGs was fabricated by UV irradiation of 4 cm long fiber section with KrF excimer laser and chromium amplitude mask with $\Lambda = 226.8$ μm. After the UV-writing, the LPGs were annealed in 150 °C for 3 hours in order to release the hydrogen, and thus stabilize the properties of the gratings [39]. After the fabrication, the LPGs were immersed in hydrofluoric acid (HF) in order to reduce the fiber cladding diameter. During that process resonant wavelength was shifted up to DTP. It is a common procedure applied for maximizing the LPG sensitivity [40]. In this experiment, highly concentrated HF (40%) and subsequently HF buffer (6 to 1 volume ratio of 40% NH_4F in water and 49% HF in water) were used. After this step the transmission spectrum of the LPG was investigated in order to determine shift of the resonance wavelength induced by etching. This process cycle was repeated several times to achieve DTP at $\lambda \sim 1600$ nm. Just before achieving DTP etching solution was changed to HF buffer in order to increase precision of the process control in determination of resonant wavelength of the LPG.

The spectral response of the LPGs was investigated in wavelength range of 1100 to 1650 nm using Yokogawa AQ6370B spectrum analyzer and Yokogawa AQ4305 white light source, and in the range of 1200 to 2250 nm using Yokogawa AQ6375 spectrum analyzer and NKT Photonics SuperK COMPACT supercontinuum white light laser source.

2.2 TiO_2 nano-films deposition and characterization

The TiO_2 thin films were deposited on the LPGs and reference silicon wafers using the TSF200 system (BENEQ, Vantaa, Finland). The reference silicon wafers went through the Radio Corporation of America cleaning procedure. The LPG samples were cleaned in isopropanol. For the TiO_2 deposition processes, water and titanium (IV) chloride ($TiCl_4$) were used as an oxygen and titanium precursors, respectively. Between gas pulses the chamber was purged with nitrogen. Thickness of the nano-films was controlled by number of cycles of the ALD process. Temperature during the process cannot be too high due to the polymer coating

#233817 - $15.00 USD Received 2 Feb 2015; revised 13 Mar 2015; accepted 16 Mar 2015; published 24 Mar 2015

of fiber cladding and it was set to 85 °C. Moreover, it is known that low deposition temperature promotes amorphous structure of TiO_2 and improves its optical properties [20].

The properties of the TiO_2 films deposited on the reference silicon wafers, such as their thickness (*d*), refractive index (*n*) and extinction coefficient (*k*) were determined by a Horiba Jobin-Yvon UVISEL spectroscopic ellipsometer. The ellipsometric model for TiO_2 analysis is described by the New Amorphous dispersion formula.

2.3 LPG measurements

The RI sensitivity was measured by immersing LPGs in mixture of water and glycerine with n_D ranging from 1.333 to 1.472 RI units (RIU). Refractive index of the liquids was measured using Rudolph J57 automatic refractometer working with resolution of $2 \cdot 10^{-5}$ RIU. Between the immersions, the LPG was rinsed with deionized water and then dried in air. Sensitivity of the LPGs was calculated as resonance wavelength shift induced by variation of RI in a specific range. Temperature and strain were kept constant during the RI measurements.

2.4 TiO_2 surface biofunctionalization

The procedure of chemical preparation of the TiO_2 surface and then protein binding comprised of the following steps. First, the fiber was immersed in the 0.01% acetic acid and 2% (3-Glycidyloxypropyl) trimethoxysilane solution in T = 90 °C for about 3 h, then it was left for about 16 h at T = 20 °C in the 0.01M $NaHCO_3$ buffer (pH = 10) with 20 mM N-(5-amino-1-carboxypentyl) iminodiacetic acid solution. Next, the sample was immersed in 10 mM $NiCl_2$ and 5 mM Glycine solution for about 2 h in room temperature. Finally, after washing in 0.01 M $NaHCO_3$ buffer the LPG was immersed in the adhesin solution with concentration of 50 μg/ml for about 1 h. The steps we followed here with TiO_2-coated LPG are similar to those described in [33,37], i.e., we use *E. coli* B bacteriophage g37 adhesin and corresponding *E. coli* B lipopolysaccharide (LPS) as a positive test for adhesin-LPS binding. However, in comparison to experiments shown in [33,37] we used slightly different functionalization procedure, i.e., lower 16 h-long process temperature (from T = 60 °C to T = 20 °C) and lower concentration of N-(5-amino-1-carboxypentyl) iminodiacetic acid. The change in long incubation process temperature and use of smaller amounts of the acid should prevent any possible damage to the thin overlay, prevent from surface etching and decrease costs of the process.

In turn, used as reference TiO_2-coated and oxidized SiO_2 wafers was immersed in green fluorescent protein (GFP) tagged with 6xHis on its N-terminus (EMD Millipore Corporation) (the procedure is specific for his-tag binding capability) for about 30 minutes, and then washed with deionized water.

3. Results and discussion

3.1 Properties of the TiO_2 nano-overlays

Thickness and optical properties of the LPG's overlay have significant influence on a spectral response of the LPG to n_{ext}. During our experiments we determined that the deposition rate reaches 0.1 nm per cycle. The result proves that the thickness of the TiO_2 films can be controlled with sub-nm precision. The dispersion curves and variation of optical properties of the TiO_2 films deposited on reference silicon wafers versus their thickness is shown in Fig. 1. Since *k* is negligible in the infrared (IR) spectral range, we focus our discussion solely on dispersion of *n*. The most significant changes in *n* of the deposited TiO_2 are seen in spectral range between 260 and 660 nm. In the investigated range of LPG response (i.e., IR), the variations of *n* are only slightly dependent on wavelength, Fig. 1(a). Furthermore, the thickness has also slight, but noticeable influence on *n* of the TiO_2 films, Fig. 1(b). The highest changes of TiO_2 *n* can be observed for its thickness below 50 nm (about 0.004 RIU/nm). With the increase of the overlay thickness above ~50 nm its optical properties

#233817 - $15.00 USD Received 2 Feb 2015; revised 13 Mar 2015; accepted 16 Mar 2015; published 24 Mar 2015

stabilize and can be assumed constant. The effect of evolution in film's *n* with its thickness has also been observed for sol-gel deposited TiO_2 [15] as well as other thin films and vapor-based deposition methods [41]. In contradiction to Al_2O_3 films, also deposited with ALD, where *n* decreases with thickness [14], at initial stage of the film growth the *n* of TiO_2 increases reaching about 2.27 RIU at λ = 1550 nm, Fig. 1(b). The increase in *n* of TiO_2 with thickness of the film may be induced by material densification [41], as well as stress induced in the film by the substrate [42]. The obtained *n* is significantly higher than for films obtained with other deposition methods [15,23,24].

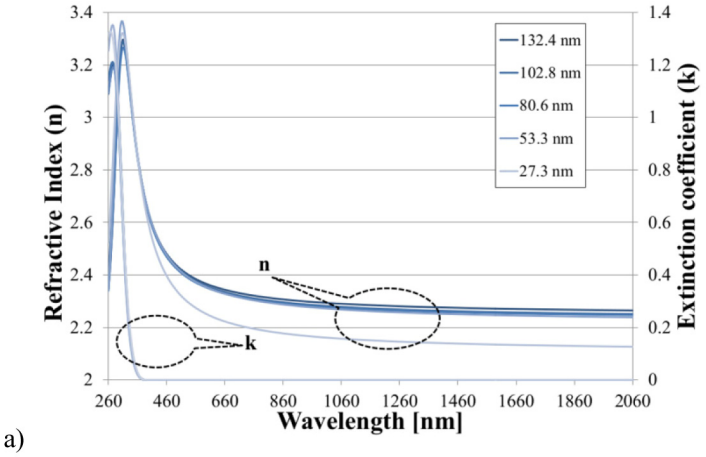

a)

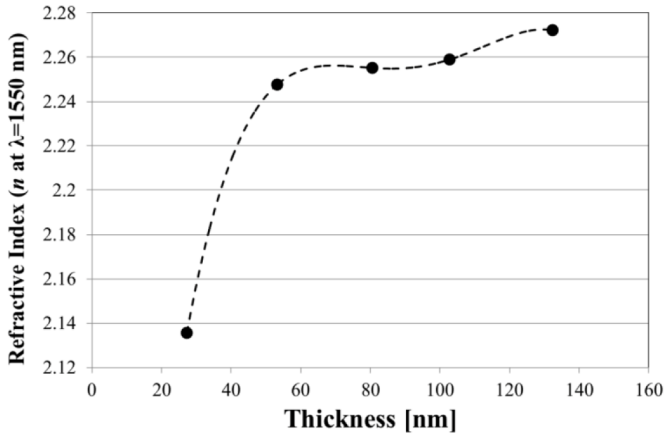

b)

Fig. 1. Influence of TiO_2 film thickness on its optical properties, where (a) shows dispersion curves of *n* and *k*, and (b) relation between *n* at λ = 1550 nm and the thickness.

3.2 RI sensitivity measurements

Measurements of the RI sensitivity for three samples were compared before and after the deposition of TiO_2, Figs. 2 and 3. In Fig. 2, it can be seen that there is a significant difference between responses of sample with and without TiO_2 overlay. For LPG sample without the overlay when it is immersed in water (n_D = 1.33302 RIU), the resonance at λ ~1600 nm is experiencing DTP. For the same sample with the thinnest overlay (*d* = 47.3 nm), the DTP repeats in the air (n_D = 1 RIU) and the resonance is shifted towards lower wavelength range as a result of immersion in water. Further, the resonance at DTP for the sample with slightly thicker overlay (*d* = 50.5 nm) is already experiencing double-resonance effect in air and then

#233817 - $15.00 USD Received 2 Feb 2015; revised 13 Mar 2015; accepted 16 Mar 2015; published 24 Mar 2015

it also shifts towards lower wavelength in water. It can be seen that thanks to high *n* of the TiO_2 overlay only couple of nm difference in its thickness strongly modifies LPG response. Interesting development of double-resonance effect is shown in Fig. 2(b), where sample with 70.0 nm thick overlay is examined. This sample, like in case of 50.5 nm thick one, already shows a double-resonance split in the air, but after immersion in water the two resonances reappear joined just before split at DTP. When the n_{ext} increases the resonances further separate in wavelength. The results prove that for high-*n* overlays only tens of nanometers in thickness are essential for full mode transition [43].

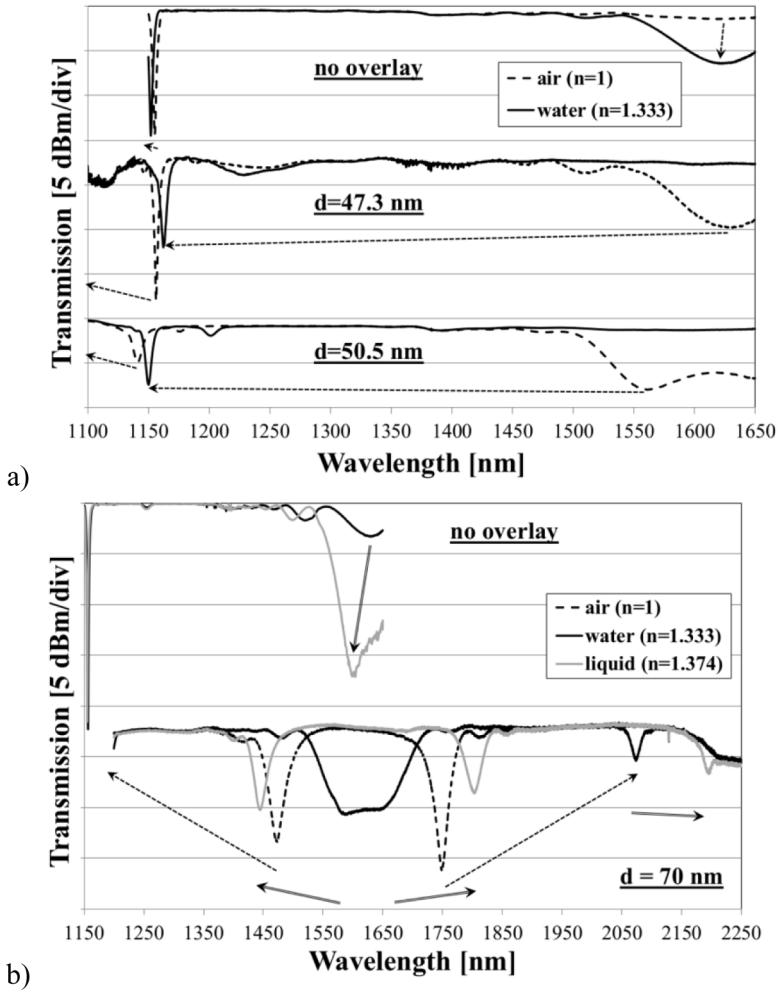

Fig. 2. Transmission spectrum of the LPG sample with and without TiO_2 overlays of different thickness (a) 47.3 nm, 50.5 nm, and (b) 70.0 nm when surrounded by air (n_D = 1 RIU), water (n_D = 1.333 RIU) and a high-RI liquid (n_D = 1.374 RIU). The arrows indicate wavelength shift induced by immersing the LPG in water (dashed) and between water and high-RI liquid (double-lined). Different spectral range shown in (b) comes from application of different optical analyzers for the sample before and after deposition.

Response of the sample with and without TiO_2 overlay to n_{ext} up to n_D = 1.47201 RIU has been investigated next. For the etched LPG with no overlay the resonance at λ~1600 nm is close to DTP up to n_{ext} ~1.36 RIU. Above this value the spectral separation of the resonance takes place and the one at lower wavelength experiences shift towards shorter wavelengths,

#233817 - $15.00 USD Received 2 Feb 2015; revised 13 Mar 2015; accepted 16 Mar 2015; published 24 Mar 2015

Fig. 3(a). It can be seen that when RI gets closer to the one of cladding material, i.e., fused silica (n_D = 1.458 RIU), cladding modes interact more with external medium and that is why the sensitivity of the device is increased [44]. For the LPGs with the TiO_2 overlay, shown in Figs. 3(b) and 3(c), there is a significant shift with n_{ext} of the resonance formed initially at λ~1600 nm and slight shift of two other resonances at about λ~1175 nm and λ~1150 nm. The shift highly depends on the overlay properties. If the overlay's n and thickness, as well as the n_{ext} are properly selected, the lowest order cladding mode starts to be guided in the overlay inducing shift of the higher order cladding modes to the nearest lower order ones [12,27,43]. When the mode transition takes place, the grating reaches the highest RI sensitivity. Comparing sensitivities of the LPGs before and after TiO_2 deposition, there can be observed a significant increase of RI sensitivity below n_{ext} = 1.44 RIU induced by the TiO_2 overlay, Fig. 4. The sensitivity to external RI for the resonance shifting in a wide spectral range can be assumed as linear for each sample in three n_{ext} ranges. In the lower RI range it is highly influenced by DTP, while for higher n_{ext} it increases as a result of mode transition effect. For d = 47.3 nm the sensitivity in n_{ext} between 1.36 and 1.41 RIU is over 4300 nm/RIU, which is over 2.2 times higher than sensitivity of a bare LPG for the resonance at the same n_{ext} range. In this range the increase in sensitivity is influenced by the operation close to the DTP. Increase in TiO_2 overlay thickness shifts the high sensitivity towards lower n_{ext} range and makes the influence of both DTP and mode transition effect more visible. For the overlay thickness of 70.0 nm, the high sensitivity range is shifted close to RI of water (n_D = 1.3330 RIU), and reaches there over 6200 nm/RIU. Similar sensitivity has been observed for LPG with no overlay where only effect induced by DTP is employed, but it reached there over 6000 nm/RIU in range only up to n_{ext} = 1.334 RIU [33]. When the LPG is coated with TiO_2, the high sensitivity range is up to n_{ext} = 1.34 RIU and covers the range used for label-free detection [33]. When n_{ext} is above 1.34 and 1.39 RIU, the sensitivity reaches 3000 and 5500 nm/RIU, respectively. In this case the sensitivity above 1.39 RIU is highly influenced by mode transition effect. For n_{ext} above 1.41 RIU, the resonance takes place of the one initially appearing at 1150 nm and the sensitivity drops down significantly. The resonance in the vicinity of 1175 nm has already experienced mode transition for samples immersed in water and takes place of the nearest lower order cladding mode. It must be noted here that thanks to combined effects of DTP and transition of higher order cladding modes, the obtained RI sensitivity is almost 19 fold higher than reported for TiO_2-coated LPGs working away from DTP [25]. The RI sensitivity shown here is according to our best knowledge both the highest and measured in the broadest RI range (close to that of water) ever reported. Higher sensitivity reported by Pilla et al. [29] has been measured for higher external RI, which is too high for label-free sensing.

#233817 - $15.00 USD Received 2 Feb 2015; revised 13 Mar 2015; accepted 16 Mar 2015; published 24 Mar 2015

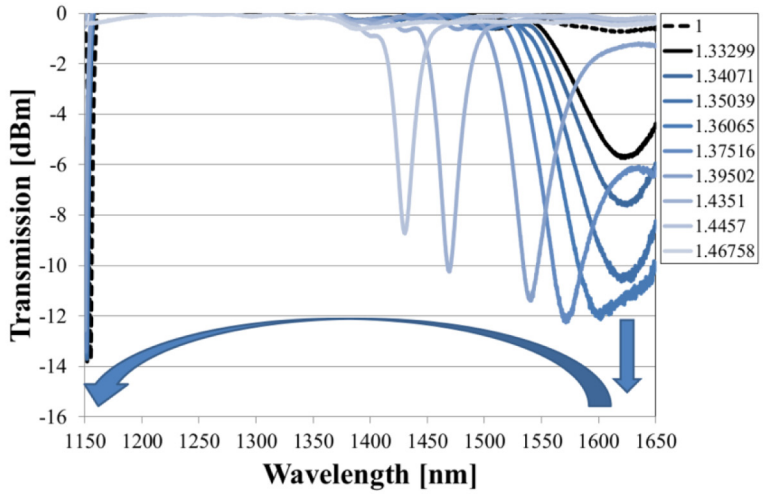

a)

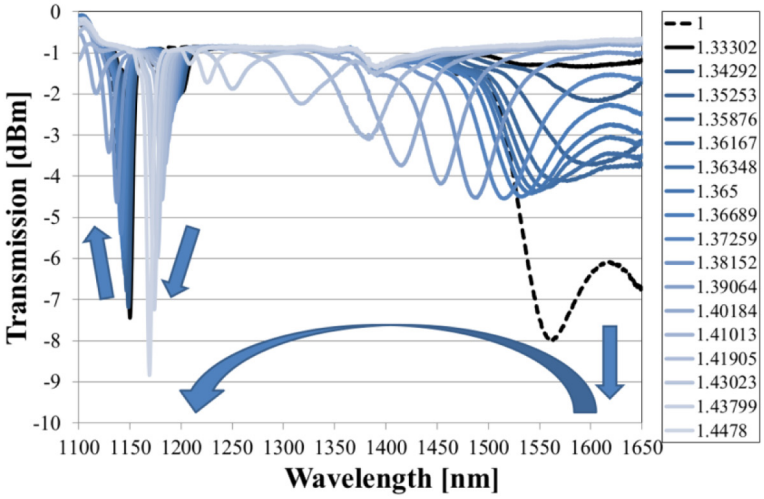

b)

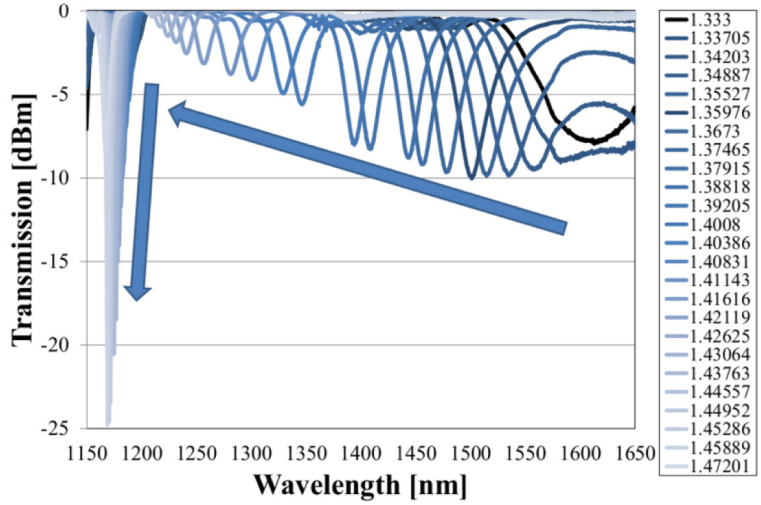

c)

#233817 - $15.00 USD Received 2 Feb 2015; revised 13 Mar 2015; accepted 16 Mar 2015; published 24 Mar 2015

Fig. 3. Evolution of tramsmission spectrum with external RI for LPG with (a) no overlay, and with (b) 50.5 and (c) 70 nm thick TiO_2 overlays.

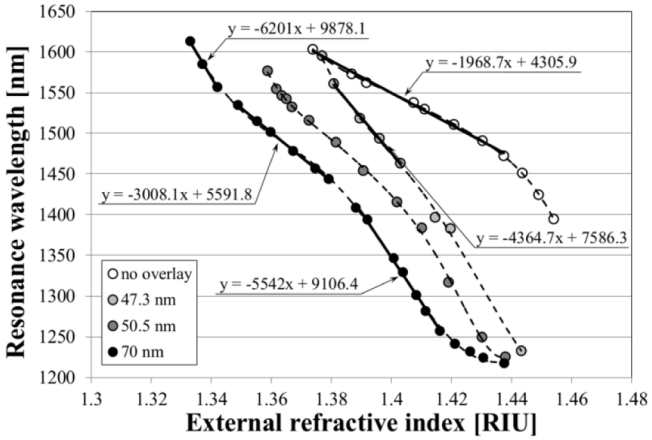

Fig. 4. Resonance wavelength shift with n_{ext} for LPG with the deposited TiO_2 of different thickness. Liner fits applied to these plots in selected n_{ext} ranges show the RI sensitivity. The estimated errors for refractive index and resonance wavelength values are $2 \cdot 10^{-5}$ RIU and 0.1 nm, respectively.

4. TiO_2 surface biofunctionalization

LPG and reference Si wafer coated with 70 nm thick TiO_2 were bio-functionalized with bacteriophage adhesin and GFP, respectively. The outcome of the experiment performed with GFP is depicted in Fig. 5, where we show photos of the functionalized sample surface with areas incubated and non-incubated in GFP. The GFP absorbs light in the spectral range of 395-425 nm and emits in green spectral region. This outcome indicates correct course of the procedure showing the binding of GFP to the TiO_2 covered surface, Fig. 5(a). Similar effect can be observed for sample coated with SiO_2, which can be treated as a good reference to other typically functionalized fiber cladding materials, Fig. 5(b).

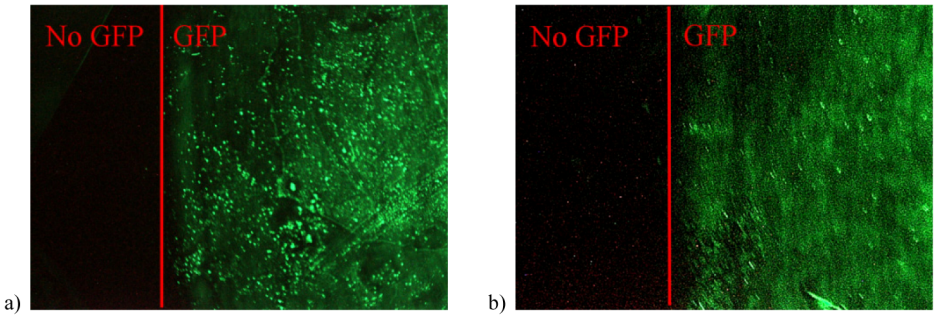

Fig. 5. Functionalized Si reference sample coated with (a) TiO_2 and (b) SiO_2. Part in both the samples was immersed in GFP and then intensively washed.

The positive results acquired for the bulk sample preceded the fiber sensor experiments which aimed to test adhesin-binding to TiO_2 surface. The results of the procedure are shown in Fig. 6, which depicts consecutive stages of the experiment after surface functionalization. In Fig. 6(b) and 6(c) the first stage, i.e., washing in $NaHCO_3$ buffer (n_D = 1.3335) has been omitted due to indistinguishable separation between two minima, Fig. 6(a). The sensor has been designed to have the two minima merged at DTP exactly at this stage of the experiment in order to achieve the highest possible sensitivity. The next step, which is incubation in bacteriophage adhesin solution, is uncovered thanks to high sensitivity. During 30 minute

#233817 - $15.00 USD Received 2 Feb 2015; revised 13 Mar 2015; accepted 16 Mar 2015; published 24 Mar 2015

incubation the process of binding adhesin to the fiber's surface is observed as continuous wavelength shift, i.e., separation of the minima, Figs. 6(b) and 6(c). The difference between signal before and after this stage is noticeable and equals to about 10 nm per side. Since bacteriophage adhesin is very small in size (the total length is just over 20 nm) [45], for its observation a high sensitivity of the sensor is desired. The effect of adhesin binding to the fiber's surface has never been observed in our earlier works where fused silica was employed as a sensor's surface [33,37].

Furthermore, it can be seen that incubation in LPS solution induced significant increase in spectral separation of the resonances, Fig. 6(a). The fiber sensor reacts to the difference in RI of PBS (n_D = 1.3346 RIU) and LPS-water solution only at the first stage of the experiment, where the value of resonance shift returns to that of water, Figs. 6(b) and 6(c). This means that the effect of RI difference is negligible and the separation of the resonances is mainly a result of binding of the LPS to bacteria adhesin which build up a thicker bio-overlay. At this stage we observe significantly higher response to LPS incubation than we have been able to do earlier. Namely, LPS incubation causes about 40 nm shift of each resonance, whilst the highest response at this stage for sensors with no TiO_2 overlay did not exceed 20 nm. Next, the extensive sample washing which followed the incubation in LPS resulted in removal of weakly, i.e., physically bound bio-material and allowed for comparison of signal responses at two stages of sample immersion in PBS. The measured shifts are 10.4 and 17.7 nm for left and right resonance, respectively. Higher shift of the right resonance has been observed before and results from longer wavelength range for this resonance [30].

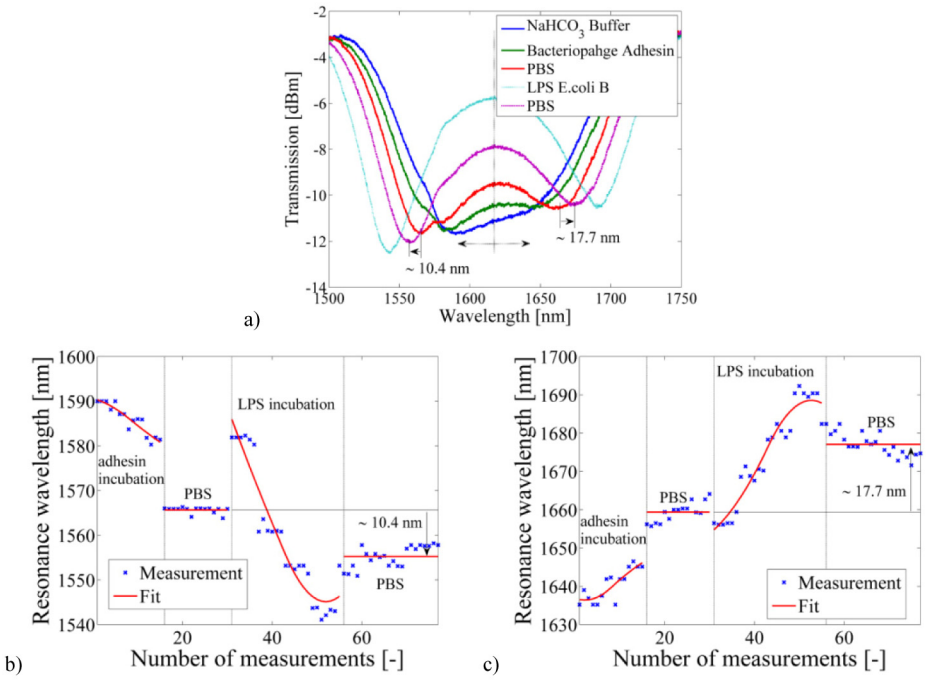

Fig. 6. Results of the adhesin-LPS binding test where (a) shows selected spectra measured before, during and after the LPS application. In figure (b) and (c) is shown wavelength shift at LPS incubation and washing steps of the experiment for left and right resonance, respectively.

Results presented in Fig. 6 are compared to those reported in [37], where fused silica surface had been functionalized. First as described above, it can be seen that the response to the immersion in LPS in case of TiO_2-coated LPG is much higher than for bare LPG. Since the RI of LPS solution, i.e. its concentration, is in both cases the same (250 μg/mL), the effect

#233817 - $15.00 USD Received 2 Feb 2015; revised 13 Mar 2015; accepted 16 Mar 2015; published 24 Mar 2015

is due to higher sensitivity in the same n_{ext} range for the TiO_2-coated sample. Next, we can see that the received difference in responses when PBS levels are compared, is only ~10 nm (Fig. 6(b)) versus ~15 nm reported in the case of the sensor without the overlay. This result can be explained by the following factors: slightly different functionalization procedure, which might have made the sensor surface less protein adhesive, and the washing procedure used in case of the fiber with overlay, which was changed from water to alternated water and $NaHCO_3$ buffer solution flows. Moreover, in this experiment we intentionally used higher flow rates to additionally test the sensor's robustness and capability of positive results in harsh testing conditions. Intensive sensor washing might have induced more material removal from the sensor's surface and thus its lower response.

Finally, taking into account the significant wavelength shift of both minima and results of the experiment with GFP presented in Fig. 5, we are convinced that the applied functionalization procedure fulfilled its task. The results prove that TiO_2-coated LPG keeps high sensitivity despite harsh biofunctionalization procedure. According to our best knowledge this work reports for the first time successful direct chemical functionalization of high-*n* overlay, which tunes sensitivity of the LPG. Up to date shown label-free sensing approaches with LPG working at mode transition employed physical adsorption of bio-molecules [46] or application of additional interfacial layer for chemical functionalization of the overlay [47].

5. Conclusions

Besides application of TiO_2 as antireflection coatings, the TiO_2 film can be successfully applied for effective tuning of RI sensitivity of LPG. The range of high RI sensitivity is determined by initial working conditions of the LPG and proper selection of number of ALD process cycles. Since the ALD method allows to determine the thickness of the overlays at a sub-nm scale, the sensitivity can be precisely tuned. Moreover, the capability of ALD process to take place at low temperatures makes it possible to deposit high-*n* TiO_2 overlays (*n* above 2.2 RIU in IR spectral range) on UV-induced LPGs without damaging the grating. Thanks to deposition of 70.0 nm thick TiO_2 overlays we obtained over 2.8 fold higher RI sensitivity for selected n_{ext} ranges than for a bare LPG. We have obtained sensitivity reaching 6200 nm/RIU in RI range up to n_{ext} = 1.34 RIU. Furthermore, taking into account significant sensitivity increase and robustness of the structure with overlay, it can be stated that the developed platform is very promising for application in label-free biosensing. We have shown successful direct chemical functionalization of the TiO_2 surface with protein receptors, and application of TiO_2-coated LPG for bacteria lipopolysaccharide detection.

Acknowledgments

The authors gratefully acknowledge support for this work from the National Centre for Research and Development of Poland within the LIDER program under grant No. LIDER/03/16/L-2/10/NCBiR/2011, National Science Centre of Poland under grant No. 2011/03/D/NZ7/02054, the Natural Sciences and Engineering Research Council of Canada, and the Canada Research Chairs Program.

#233817 - $15.00 USD Received 2 Feb 2015; revised 13 Mar 2015; accepted 16 Mar 2015; published 24 Mar 2015